

FTUAM 02/11
 IFT-UAM/CSIC-02-11
 HIP-2002-17/TH
 hep-ph/0204271
 April 2002

Experimental Constraints on the Neutralino-Nucleon Cross Section*

D.G. CERDEÑO¹, E. GABRIELLI², C. MUÑOZ¹

¹ *Departamento de Física Teórica C-XI and Instituto de Física Teórica C-XVI,
 Universidad Autónoma de Madrid, Cantoblanco, 28049 Madrid, Spain.*

² *Helsinki Institute of Physics, P.O. Box 64, FIN-00014 Helsinki, Finland.*

In the light of recent experimental results for the direct detection of dark matter, we analyze in the framework of SUGRA the value of the neutralino-nucleon cross section. We study how this value is modified when the usual assumptions of universal soft terms and GUT scale are relaxed. In particular we consider scenarios with non-universal scalar and gaugino masses and scenarios with intermediate unification scale. We also study superstring constructions with D-branes, where a combination of the above two scenarios arises naturally. In the analysis we take into account the most recent experimental constraints, such as the lower bound on the Higgs mass, the $b \rightarrow s\gamma$ branching ratio, and the muon $g - 2$.

1 Introduction

One of the most interesting candidates for dark matter is a long-lived or stable weakly-interacting massive particle (WIMP). WIMPs can remain from the earliest moments of the Universe in sufficient number to account for a significant fraction of relic density. These particles would form not only a background density in the Universe, but also would cluster gravitationally with ordinary stars in the galactic halos. This raises the hope of detecting relic WIMPs directly, by observing their elastic scattering on target nuclei through nuclear recoils [1]. In fact, one of the current experiments, the DAMA collaboration, reported recently [2] data favoring the existence of a WIMP signal. It was claimed that (at 4σ C.L.) the preferred range of the WIMP-nucleon cross section is 10^{-6} - 10^{-5} pb for a WIMP mass between 30 and 200 GeV. Unlike this spectacular result, other collaborations, CDMS [3], EDELWEISS [4], and IGEX [5], claim to have excluded regions of the DAMA parameter space.

In any case, due to these and other projected experiments, it seems very plausible that the dark matter will be found in the near future. In this situation, and assuming

*Talk given at Corfu Summer Institute on Elementary Particle Physics, August 31-September 20, 2001.

that the dark matter is a WIMP, it is natural to wonder how big the cross section for its direct detection can be. The answer to this question depends on the particular WIMP considered. The leading candidate in this class is the lightest neutralino [1], a particle predicted by the supersymmetric (SUSY) extension of the standard model (SM).

In the simplest SUSY extension, the so-called minimal supersymmetric standard model (MSSM), there are four neutralinos, $\tilde{\chi}_i^0$ ($i = 1, 2, 3, 4$), since they are the physical superpositions of the bino (\tilde{B}^0), of the neutral wino (\tilde{W}_3^0), and of the neutral Higgsinos ($\tilde{H}_u^0, \tilde{H}_d^0$). In most of the parameter space of the MSSM, the lightest neutralino, $\tilde{\chi}_1^0$, is the lightest supersymmetric particle (LSP). When R-parity is imposed this implies that $\tilde{\chi}_1^0$ is absolutely stable, and therefore a dark matter candidate.

In this paper we will analyze this SUSY scenario in the framework of supergravity (SUGRA), and in particular several constructions proposed recently in the literature (for a review see ref. [6]), where the $\tilde{\chi}_1^0$ -nucleon cross section can be enhanced, and might be of the order of 10^{-6} pb, i.e., where current dark matter detectors are sensitive. First, in Section 2, we will briefly introduce the SUGRA framework. In Section 3 we will describe the most recent experimental constraints which can affect the computation of the cross section. Then, in the rest of the sections, we will re-evaluate previous computations, taking into account these constraints. In particular, in Section 4 we will review the value of the cross section when universal soft SUSY-breaking terms are assumed, and how this value is modified when this assumption is relaxed [7, 8, 9, 6, 10]. In Section 5 we will consider the case of an intermediate unification scale [11, 12]. Finally, in Section 6, we will study superstring scenarios with D-branes [13].

2 SUGRA framework

Working in the framework of SUGRA one makes several assumptions. In particular, the soft parameters, i.e., gaugino masses, scalar masses, and trilinear couplings, are generated once SUSY is broken through gravitational interactions. They are denoted at the grand unification scale, $M_{GUT} \approx 2 \times 10^{16}$ GeV, by M_a , m_α , and $A_{\alpha\beta\gamma}$ respectively. Likewise, radiative electroweak symmetry breaking is imposed, i.e., the Higgsino mass parameter μ is determined by the minimization of the Higgs effective potential. This implies

$$\mu^2 = \frac{m_{H_d}^2 - m_{H_u}^2 \tan^2 \beta}{\tan^2 \beta - 1} - \frac{1}{2} M_Z^2, \quad (1)$$

where $\tan \beta = \langle H_u^0 \rangle / \langle H_d^0 \rangle$ is the ratio of Higgs vacuum expectation values.

The soft SUSY-breaking terms will have in general a non-universal structure in the framework of SUGRA [14]. For the case of the observable scalar masses, this is due to the non-universal couplings in the Kähler potential between the hidden sector fields breaking SUSY and the observable sector fields. For the case of the gaugino masses, this is due to the non-universality of the gauge kinetic functions associated to the different gauge groups. Explicit string constructions, whose low-energy limit is SUGRA, exhibit these properties [14].

With these assumptions, the SUGRA framework still allows a large number of free parameters. In particular, it contains more than 100 parameters. In order to have predictive power one usually assumes in addition that the above soft parameters are real and universal at M_{GUT} . This is the so-called minimal supergravity (mSUGRA) scenario, where there are only four free parameters: m , M , A , and $\tan\beta$. In addition, the sign of μ remains also undetermined. It is worth noticing that explicit string constructions with these characteristics can also be found [14].

3 Experimental constraints

Here we list the most recent experimental results which might be relevant when computing the $\tilde{\chi}_1^0$ -nucleon cross section in the context of SUGRA. In particular, they may produce important constraints in the parameter space, forbidding for example points with a large cross section.

- Higgs mass

Whereas in the context of the SM, the negative direct search for the Higgs at the LEP2 collider implies a precise lower bound on its mass of 114.1 GeV, the situation in SUSY scenarios is more involved. In particular, in the framework of mSUGRA, one obtains [15] for the lightest CP-even Higgs mass $m_h \gtrsim 114.1$ GeV when $\tan\beta \lesssim 50$, and $m_h \gtrsim 91$ GeV when $\tan\beta$ is larger. Let us remark that $\tan\beta$ is constrained to be smaller than 60 since otherwise the condition of radiative electroweak symmetry breaking cannot be fulfilled.

On the other hand, when the mSUGRA framework is relaxed the above SUSY bounds must be modified. In particular, for the benchmark scenarios studied in ref. [16] one obtains $m_h \gtrsim 114.1$ GeV when $\tan\beta \lesssim 8$, and $m_h \gtrsim 91$ GeV when $\tan\beta$ is larger.

Let us finally remark that in our computation below we evaluate m_h using the program *FeynHiggsFast*, a simplified version of the updated program *FeynHiggs* [17] which contains the complete one-loop and dominant two-loop corrections. The value of m_h obtained with *FeynHiggsFast* is approximately 1 GeV below the one obtained using *FeynHiggs*. In addition, we should also keep in mind that the value of m_h obtained with *FeynHiggs* has an uncertainty of about 3 GeV, due e.g. to higher-order corrections.

- Top mass

Needless to say we use as input for the top mass throughout this paper the central experimental value $m_t(\text{pole}) = 175$ GeV. However, let us remark that a modification in this mass by ± 1 GeV implies, basically, a modification also of ± 1 GeV in m_h .

- SUSY spectrum

We impose the present experimental lower bounds on SUSY masses coming from LEP and Tevatron. In particular, using the low-energy relation from mSUGRA, $M_1 = \frac{5}{3} \tan^2 \theta_W M_2$, one obtains for the lightest chargino mass the bound [18] $m_{\tilde{\chi}_1^\pm} > 103$ GeV. Likewise, one is also able to obtain the following bounds for sleptons masses [19]: $m_{\tilde{e}} > 99$ GeV, $m_{\tilde{\mu}} > 96$ GeV, $m_{\tilde{\tau}} > 87$ GeV. Finally, we use the following bounds on the masses of sneutrino, the stop, the rest of squarks, and gluinos: $m_{\tilde{\nu}} > 50$ GeV, $m_{\tilde{t}} > 95$ GeV, $m_{\tilde{q}} > 150$ GeV, $m_{\tilde{g}} > 190$ GeV.

- $b \rightarrow s\gamma$

The measurements of $B \rightarrow X_s \gamma$ decays at CLEO [20] and BELLE [21], lead to bounds on the branching ratio $b \rightarrow s\gamma$. In particular we impose in our computation $2 \times 10^{-4} \leq BR(b \rightarrow s\gamma) \leq 4.1 \times 10^{-4}$, where the evaluation is carried out at the NLO accuracy in the SM [22], while for the SUSY contributions only the 1-loop diagrams have been taken into account [23].

- $g_\mu - 2$

The new measurement of the anomalous magnetic moment of the muon, $a_\mu = (g_\mu - 2)/2$, in the E821 experiment at the BNL [24] implied apparently a 2.6σ deviation from the SM predictions. In particular, taking a 2σ range around the E821 central value one would have $11 \times 10^{-10} \leq a_\mu(E821) - a_\mu(SM) \leq 75 \times 10^{-10}$. However, recent theoretical computations [25] have shown that a significant part of this discrepancy was due to the evaluation of the hadronic light-by-light contribution [26]. As a consequence, assuming that the possible new physics is due to SUGRA, we impose in our computation the current constraint $-7 \times 10^{-10} \leq a_\mu(SUGRA) \leq 57 \times 10^{-10}$ at the 2σ level.

- LSP

The LSP must be an electrically neutral (also with no strong interactions) particle, since otherwise it would bind to nuclei and would be excluded as a candidate for dark matter from unsuccessful searches for exotic heavy isotopes [27]. As mentioned in the Introduction, the $\tilde{\chi}_1^0$ is the LSP in most of the parameter space of SUGRA. However, in some regions the stau can be lighter than the $\tilde{\chi}_1^0$. Following the above argument, we discard these regions.

Other cosmological constraints, as e.g. the observational bounds on the relic $\tilde{\chi}_1^0$ density, $0.1 \lesssim \Omega_{\tilde{\chi}_1^0} h^2 \lesssim 0.3$, will not be applied. The computation of the relic $\tilde{\chi}_1^0$ density depends on assumptions about the evolution of the early Universe, and therefore different cosmological scenarios give rise to different results [28].

4 SUGRA predictions for the neutralino-nucleon cross section

The cross section for the elastic scattering of $\tilde{\chi}_1^0$ on nucleons has been examined exhaustively in the literature (for a recent re-evaluation see ref. [29]). Let us recall that

the relevant effective Lagrangian describing the elastic scattering of $\tilde{\chi}_1^0$ on protons and neutrons has a spin-independent (scalar) interaction and a spin-dependent interaction. However, the contribution of the scalar one is generically larger and therefore we will concentrate on it. This scalar interaction includes contributions from squark exchange and neutral Higgs exchange. Let us also remark that the scalar cross sections for both, protons and neutrons, are basically equal.

In what follows we will review the possible value of the cross section in the framework of SUGRA. First we will consider the mSUGRA scenario, where the soft terms are assumed to be universal, and we will later relax this condition allowing non-universal soft masses.

4.1 mSUGRA scenario

In the mSUGRA scenario $\tilde{\chi}_1^0$ is mainly bino. This result can be qualitatively understood from the well known evolution of $m_{H_u}^2$ with the scale. It becomes large and negative at low scales. Then $|\mu|$ given by eq. (1) becomes also large, and in particular much larger than M_1 and M_2 . Thus, the lightest neutralino will be mainly gaugino, and in particular bino, since, as mentioned in the previous section, at low energy $M_1 = \frac{5}{3} \tan^2 \theta_W M_2 \approx 0.5 M_2$.

When $\tilde{\chi}_1^0$ is basically bino scattering channels through Higgs (h , H) exchange are highly suppressed, and as a consequence, the predicted scalar $\tilde{\chi}_1^0$ -proton cross section is well below the accessible experimental regions for low and moderate values of $\tan \beta$ [29]. Although the cross section increases entering in the DAMA region [2, 31] when the value of $\tan \beta$ increases [7, 8], the experimental constraints discussed in Section 3 exclude this possibility [30, 10]. We show this fact in Fig. 1. There the $\tilde{\chi}_1^0$ -proton cross section $\sigma_{\tilde{\chi}_1^0-p}$ as a function of the neutralino mass $m_{\tilde{\chi}_1^0}$ for $\tan \beta = 20$ and 35 is plotted.

Concerning the parameter space of the figure, we use the following values. For the soft scalar mass $0 \leq m \leq 600$ GeV, where the curve associated to $m = 600$ GeV corresponds to the minimum values of $\sigma_{\tilde{\chi}_1^0-p}$ in the figure. Note that in order to avoid the stau being the LSP not very small values of m are in fact allowed. The cross section is not very sensitive to the specific values of A in a wide range. In particular, we have checked that this is so for $|A/M| \lesssim 4$. In the figure we fix $A = M$, corresponding to the maximum value of $\sigma_{\tilde{\chi}_1^0-p}$. On the other hand, the gaugino mass M is essentially fixed for a given $\tan \beta$ and $m_{\tilde{\chi}_1^0}$. We consider only positive values of M , since negative ones correspond to smaller cross sections. Finally, we choose to plot only the case $\mu > 0$ since for negative values of μ the cross section is smaller. In addition, constraints coming from the $b \rightarrow s\gamma$ and $g_\mu - 2$ processes highly reduce the $\mu < 0$ parameter space. Let us remark that we are using the conventions for the SUGRA parameters entering in the Lagrangian explained in ref. [6].

Concerning the experimental constraints, the lower bound in the figure $m_{\tilde{\chi}_1^0} \gtrsim 50$ GeV is obtained imposing the experimental bound on the lightest chargino mass $m_{\tilde{\chi}_1^\pm} > 90$ GeV. However, as mentioned in Section 3, the most recent bound in the context of mSUGRA is now [18] $m_{\tilde{\chi}_1^\pm} > 103$ GeV, and we show it with a dotted line. We also show in Fig. 1 several values of the Higgs mass with dashed lines. In addition the

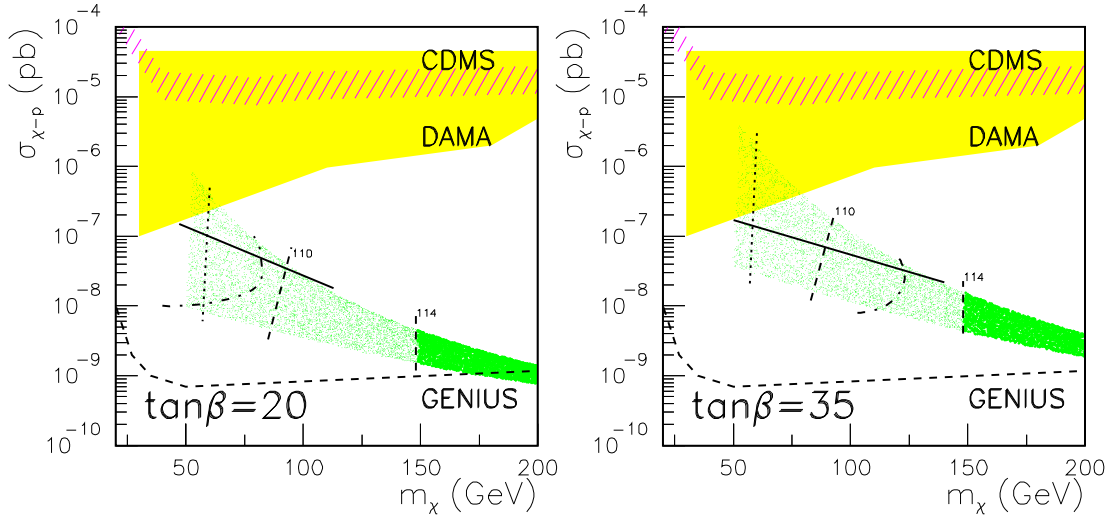


Figure 1: Scatter plot of the neutralino-proton cross section $\sigma_{\tilde{\chi}_1^0-p}$ as a function of the neutralino mass $m_{\tilde{\chi}_1^0}$ in the mSUGRA scenario, for $\tan\beta = 20$ and 35 . The dotted line corresponds to the LEP lower bound $m_{\tilde{\chi}_1^\pm} = 103$ GeV. Dashed lines correspond to different values of the Higgs mass, 110 and 114 GeV. The region to the left of the dot-dashed curve is excluded by $b \rightarrow s\gamma$, and the region above the solid line is excluded by $g_\mu - 2$. DAMA and CDMS current experimental limits and projected GENIUS limits are shown.

region to the left of the dot-dashed curve is excluded by $b \rightarrow s\gamma$, and the region above the solid line is excluded by $g_\mu - 2$.

As we can see, the present experimental lower limit for the Higgs mass in mSUGRA when $\tan\beta \lesssim 50$, $m_h \gtrsim 114.1$ GeV, is the most important constraint, implying that only the solid region where $\sigma_{\tilde{\chi}_1^0-p} \lesssim 10^{-8}$ pb survives. Obviously, in this mSUGRA case, more sensitive detectors producing further data are needed. Fortunately, many dark matter detectors are being projected. Particularly interesting is the GENIUS detector [32], where values of the cross section as low as 10^{-9} pb will be accessible, as shown in the figure.

Very large values of $\tan\beta$, like $\tan\beta \simeq 50$, have also been considered [33, 30, 10]. Although it was found, as expected, that the cross section is enhanced, the well known experimental limits coming from $b \rightarrow s\gamma$ for large $\tan\beta$, lead to severe constraints on the parameter space. In particular, these constraints imply $\sigma_{\tilde{\chi}_1^0-p} \lesssim 10^{-7}$ pb.

4.2 Scenario with non-universal soft terms

It was shown recently that non-universality allows to increase the neutralino-proton cross section. The key point consists of reducing the value of $|\mu|$. Following the discussion in the previous subsection, the smaller $|\mu|$ is, the larger the Higgsino components of the lightest neutralino become. Eventually, $|\mu|$ will be of the order of M_1 , M_2 and $\tilde{\chi}_1^0$ will be a mixed Higgsino-gaugino state. Indeed scattering channels through Higgs

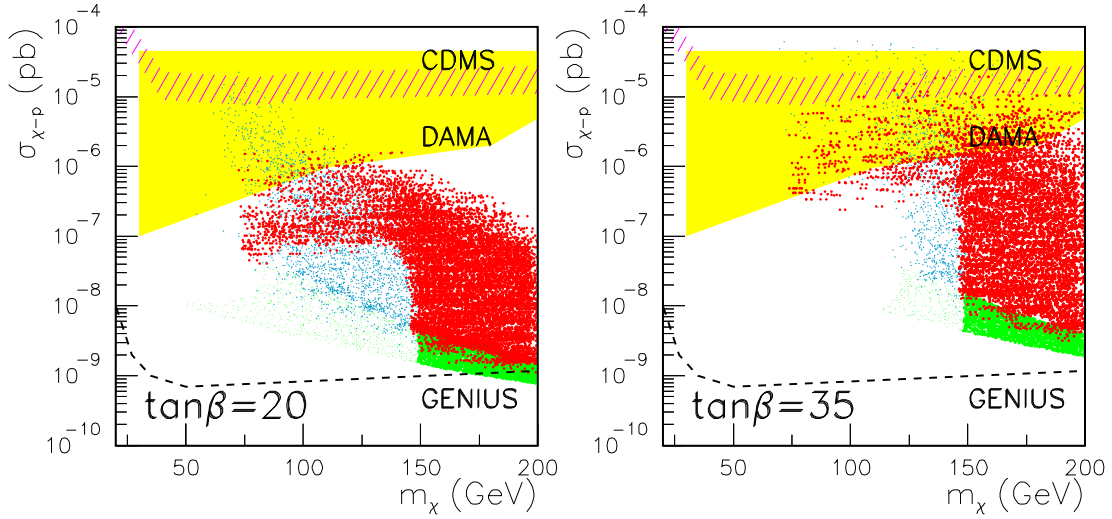


Figure 2: Scatter plot of the neutralino-proton cross section $\sigma_{\tilde{\chi}_1^0-p}$ as a function of the neutralino mass $m_{\tilde{\chi}_1^0}$ in the SUGRA scenario with non-universal soft scalar masses, for $\tan\beta = 20$ and 35. Only points of the parameter space fulfilling $b \rightarrow s\gamma$ and $g_\mu - 2$ are plotted. Big (red) dots correspond to points with $m_h \geq 114$ GeV. Small (blue) dots correspond to points with $91 < m_h < 114$ GeV. The universal case (green region) is shown for comparison. DAMA and CDMS current experimental limits and projected GENIUS limits are also shown.

exchange are now important and their contributions to the cross section will increase it. This can be carried out with non-universal scalar masses [7, 8, 10] and/or gaugino masses [9, 6].

We can have a qualitative understanding from the following. When $m_{H_u}^2(m_{H_d}^2)$ at M_{GUT} increases(decreases), its negative(positive) contribution at low energy in eq. (1) is less important. Likewise, when $m_{Q_L}^2$ and $m_{u_R}^2$ at M_{GUT} decrease, due to their contribution proportional to the top Yukawa coupling in the RGE of $m_{H_u}^2$ the negative contribution of the latter to μ^2 is again less important.

This effect can be seen in Fig. 2, where a scatter plot of $\sigma_{\tilde{\chi}_1^0-p}$ as a function of $m_{\tilde{\chi}_1^0}$ for a scanning of the soft scalar masses is shown. This scanning is explained in detail e.g. in ref. [6]. As in Fig. 1, we are taking $A = M$. For comparison we superimpose also the region (green area) obtained in Fig. 1 with universality. We see that non-universal scalar masses help in increasing the value of $\sigma_{\tilde{\chi}_1^0-p}$. In the figure we only plot the points of the parameter space fulfilling $b \rightarrow s\gamma$ and $g_\mu - 2$. In particular, the big (red) dots correspond to points with $m_h \geq 114$ GeV. As a conservative approach, we also plot with small (blue) dots those points with $91 < m_h < 114$ GeV (as discussed in Section 3, this possibility may arise when the mSUGRA scenario is relaxed). For $\tan\beta = 20$, both kind of points enter in the DAMA region. In particular, those with $m_h < 114$ GeV have an upper bound for the cross section $\approx 10^{-5}$ pb, whereas for those with $m_h > 114$ GeV the upper bound is $\approx 10^{-6}$ pb. For $\tan\beta = 35$, the area of points entering in the DAMA region increases a lot, and now, even points with $m_h > 114$

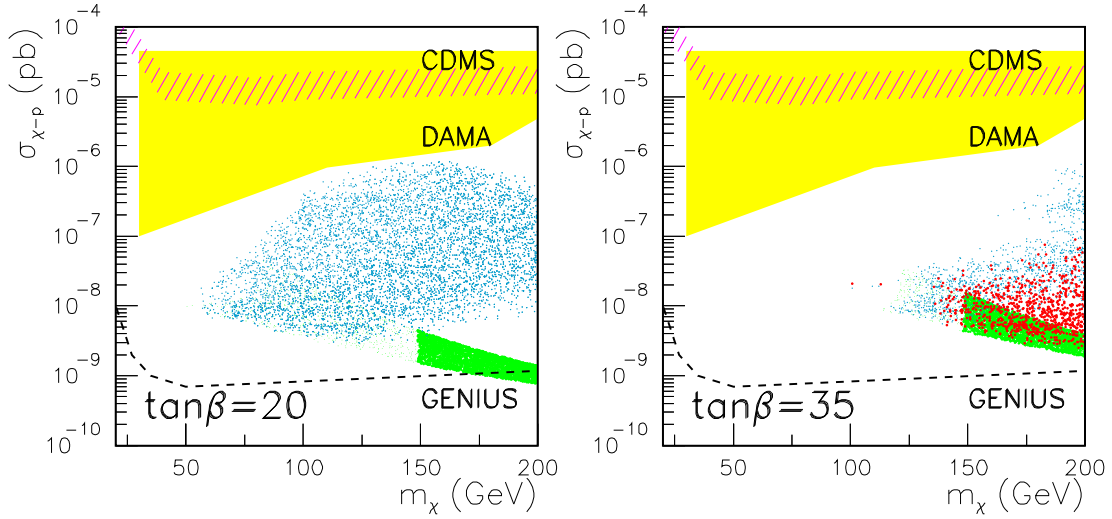


Figure 3: The same as in Fig. 2 but using non-universal soft gaugino masses.

GeV can have $\sigma_{\tilde{\chi}_1^0-p} \approx 10^{-5}$ pb. Let us finally remark that the non-universality in the Higgs sector gives the most important effect, and the non-universality in the sfermion sector only increases slightly the cross section.

On the other hand, concerning gaugino masses, it is worth noticing that M_3 appears in the RGEs of squark masses, so e.g. their contribution proportional to the top Yukawa coupling in the RGE of $m_{H_u}^2$ will do this less negative if M_3 is small, and therefore μ^2 will become smaller in this case. Taking into account this effect, we show in Fig. 3, for $\tan \beta = 20$ and 35, a scatter plot of $\sigma_{\tilde{\chi}_1^0-p}$ as a function of $m_{\tilde{\chi}_1^0}$ for the scanning of the parameters M_3, M_2, M_1 explained in ref. [6]. Although points with a large cross section entering in the DAMA region do exist [6], they are, at the end of the day, forbidden when $b \rightarrow s\gamma$ and $g_\mu - 2$ constraints are imposed.

Clearly, in this sense, SUGRA scenarios with non-universal scalars are favored with respect to scenarios with non-universal gauginos.

5 Scenario with intermediate unification scale

The analyses of $\sigma_{\tilde{\chi}_1^0-p}$ in SUGRA, described in the previous section, were performed assuming the unification scale $M_{GUT} \approx 10^{16}$ GeV. However, there are several interesting arguments in favor of SUGRA scenarios with scales $M_I \approx 10^{10-14}$ GeV. These can be found e.g. in ref. [6] and references therein. Thus to use the value of the initial scale, say M_I , as a free parameter for the running of the soft terms is particularly interesting. In this sense, it was recently pointed out [11] that $\sigma_{\tilde{\chi}_1^0-p}$ is very sensitive to the variation of the initial scale for the running of the soft terms. For instance, by taking $M_I = 10^{10-12}$ GeV rather than M_{GUT} , regions in the parameter space of mSUGRA can be found where $\sigma_{\tilde{\chi}_1^0-p}$ is two orders of magnitude larger than for M_{GUT} .

The fact that smaller initial scales imply a larger $\sigma_{\tilde{\chi}_1^0-p}$ can be understood from the

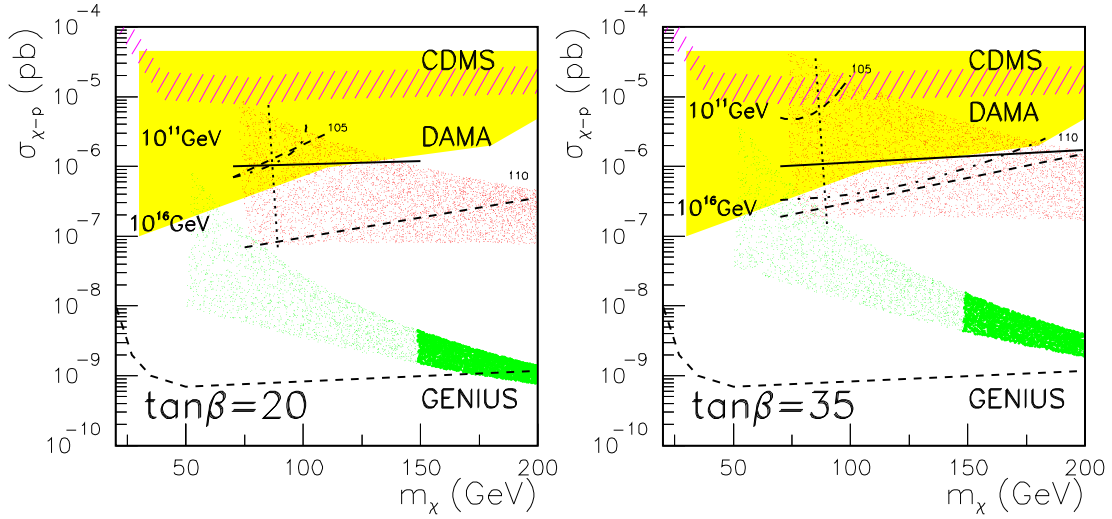


Figure 4: The same as in Fig. 1 but including the case with intermediate scale, $M_I = 10^{11}$ GeV. Now the Higgs masses 105 and 110 GeV are shown.

variation in the value of μ with M_I . One observes that, for $\tan \beta$ fixed, the smaller the initial scale for the running is, the smaller the numerator in the first piece of eq.(1) becomes. This can be understood qualitatively from the well known evolution of $m_{H_d}^2$ and $m_{H_u}^2$ with the scale. Clearly, the smaller the initial scale is, the shorter the running becomes. As a consequence, also the less important the positive(negative) contribution $m_{H_d}^2(m_{H_u}^2)$ to μ^2 in eq.(1) becomes. Thus $|\mu|$ decreases, and therefore, as discussed in the previous section, $\sigma_{\tilde{\chi}_1^0-p}$ increases. This is shown in Fig. 4, where the result for the scale $M_I = M_{GUT}$ is compared with the result for the intermediate scale $M_I = 10^{11}$ GeV.

Clearly, in the latter scenario the Higgs mass decreases and all points would be excluded if we impose the mSUGRA bound $m_h > 114$ GeV. On the other hand, taking into account the conservative approach discussed in Section 3, since all points in the figure have $m_h > 100$ GeV we will not discard them. Then, the most important constraint for $\tan \beta = 20$ is due to $g_\mu - 2$, excluding a large area of points in the DAMA region. We can understand this from the results of ref. [34]. There, a_μ versus $m_{\tilde{\chi}_1^0}$ is plotted, and one can observe that for $m_{\tilde{\chi}_1^0} \leq 150$ GeV and m small too large values of a_μ , beyond the experimental upper bound, are obtained. Note that the area left in DAMA by this constraint and the mSUGRA one $m_{\tilde{\chi}_1^\pm} > 103$ GeV may be increased if we relaxed the latter bound to e.g. 90 GeV. We see in Fig. 4 that the range $75 \text{ GeV} \lesssim m_{\tilde{\chi}_1^0} \lesssim 125 \text{ GeV}$ is now consistent with DAMA limits. However, for $\tan \beta = 35$ all points in the DAMA region are excluded because of $b \rightarrow s\gamma$.

Given the above situation concerning the enhancement of the neutralino-proton cross section through non-universal scalars and intermediate scales, it is worth analyzing the combination of both possibilities. This is shown in Fig. 5. Although no points with $m_h > 114$ GeV enter in the DAMA region, many points with $91 < m_h < 114$ GeV do enter and are allowed by all the other constraints. For $\tan \beta = 35$ the allowed

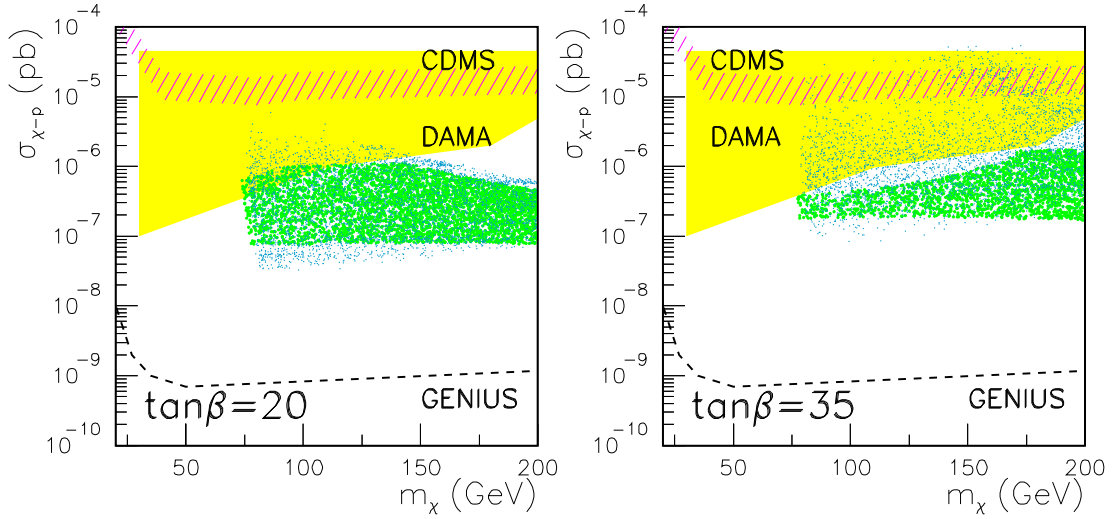


Figure 5: Scatter plot of the neutralino-proton cross section $\sigma_{\tilde{\chi}_1^0-p}$ as a function of the neutralino mass $m_{\tilde{\chi}_1^0}$ in the SUGRA scenario with the intermediate scale $M_I = 10^{11}$ GeV and non-universal soft scalar masses, for $\tan\beta = 20$ and 35. Only points of the parameter space fulfilling $b \rightarrow s\gamma$ and $g_\mu - 2$ are plotted. (Blue) dots correspond to points with $91 < m_h < 114$ GeV. The universal case (green region) is shown for comparison. DAMA and CDMS current experimental limits and projected GENIUS limits are also shown.

area is extremely large and we can even have points entering in the region excluded by CDMS.

6 Superstring scenario with D-branes

In the previous section the analyses were performed assuming intermediate unification scales. In fact, this situation can be inspired by superstring theories, since it was recently realized that the string scale may be anywhere between the weak and the Plank scale. For example, embedding the SM inside D3-branes in type I strings, the string scale is given by $M_I^4 = \alpha M_{Plank} M_c^3 / \sqrt{2}$, where α is the gauge coupling and M_c is the compactification scale. Thus one gets $M_I \approx 10^{10-12}$ GeV with $M_c \approx 10^{8-10}$ GeV. In addition, D-brane constructions are explicit scenarios where not only intermediate scales arise naturally but also non-universality.

The crucial point in these analyses is the D-brane origin of the $U(1)_Y$ gauge group as a combination of other $U(1)$'s, and its influence on the matter distribution in these scenarios. In particular, scenarios with the gauge group and particle content of the SUSY SM lead naturally to intermediate values for the string scale, in order to reproduce the value of gauge couplings deduced from experiments. In addition, the soft terms turn out to be generically non-universal. Due to these results, large cross sections can be obtained [13].

Let us consider for example a type I string scenario where the gauge group $U(3) \times$

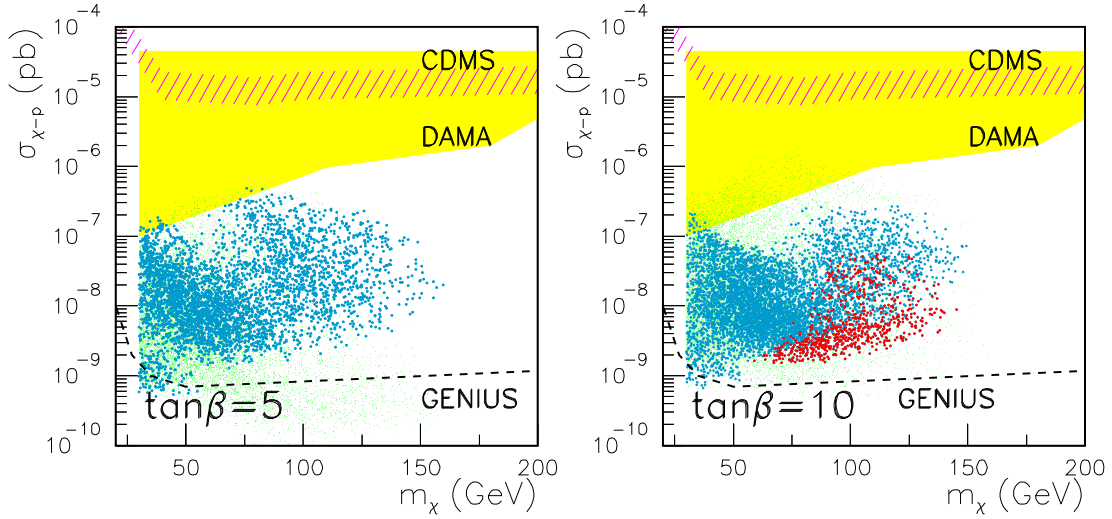


Figure 6: Scatter plot of the neutralino-proton cross section $\sigma_{\tilde{\chi}_1^0-p}$ as a function of the neutralino mass $m_{\tilde{\chi}_1^0}$ in the D-brane scenario with the string scale $M_I = 10^{12}$ GeV discussed in the text, and for $\tan\beta = 10$ and 15 . Only the big (red and blue) dots fulfil $b \rightarrow s\gamma$ and $g_\mu - 2$ constraints. The red ones correspond to points with $m_h \geq 114$ GeV whereas the blue ones correspond to points with $91 < m_h < 114$ GeV. DAMA and CDMS current experimental limits and projected GENIUS limits are also shown.

$U(2) \times U(1)$, giving rise to $SU(3) \times SU(2) \times U(1)^3$, arises from three different types of D-branes, and therefore the gauge couplings are non-universal. Here $U(1)_Y$ is a linear combination of the three $U(1)$ gauge groups arising from $U(3)$, $U(2)$ and $U(1)$ within the three different D-branes. As shown in ref. [13], this leads to the string scale $M_I = 10^{12}$ GeV. Likewise, assuming that only the dilaton (S) and moduli (T_i) fields contribute to SUSY breaking, it was found that the soft terms are generically non-universal.

Fig. 6 displays a scatter plot of $\sigma_{\tilde{\chi}_1^0-p}$ as a function of the neutralino mass $m_{\tilde{\chi}_1^0}$ for a scanning of the parameter space described in ref. [13]. In particular, the gravitino mass $m_{3/2} \leq 300$ GeV is taken, since larger values will always produce a cross section below DAMA limits. The cases $\tan\beta = 10$ and 15 are shown in Fig. 6. Although regions of the parameter space consistent with DAMA limits exist, the $b \rightarrow s\gamma$ and $g_\mu - 2$ constraints forbid most of them. The latter are shown with small (green) points, and they have $91 < m_h < 114$ GeV. For example, to understand this result for $g_\mu - 2$ is simple. In ref. [34] a_μ versus $m_{3/2}$ is plotted, and one can observe that for $m_{3/2} \lesssim 300$ GeV too large values of a_μ , beyond the experimental upper bound, are obtained. In Fig. 6 only regions with big (red and blue) dots fulfil the above mentioned constraints. The red ones correspond to points with $m_h \geq 114$ GeV whereas the blue ones correspond to points with $91 < m_h < 114$ GeV. It is worth noticing that the larger $\tan\beta$ is, the smaller the regions allowed by the experimental constraints become. For example, increasing $\tan\beta$ the value of a_μ turns out to be larger and may exceed the experimental bounds.

7 Conclusions

We have reviewed the direct detection of supersymmetric dark matter in the light of recent experimental results. They require a large cross section of the order of 10^{-6} pb. Although in the context of the mSUGRA scenario one cannot obtain this value once the experimental constraints are imposed, this is possible for other scenarios. This is the case of SUGRA models with non-universal soft scalar masses. Likewise, scenarios with intermediate unification scale may also produce this value if some experimental bounds are relaxed.

Acknowledgements

We thank S. Khalil and E. Torrente-Lujan as co-authors of some of the works reported in this paper. D.G. Cerdeño acknowledges the financial support of the Comunidad de Madrid through a FPI grant. E. Gabrielli is grateful to the CERN Theory Division and the Department of Theoretical Physics of Madrid Autónoma University, where part of this work has been done, for their warm hospitality. The work of C. Muñoz was supported in part by the Ministerio de Ciencia y Tecnología under contract FPA2000-0980, and the European Union under contract HPRN-CT-2000-00148.

References

- [1] For a recent review, see, S. Khalil and C. Muñoz, Contemp. Phys. 43 (2002) 51, hep-ph/0110122.
- [2] DAMA Collaboration, R. Bernabei et al., Phys. Lett. B480 (2000) 23.
- [3] CDMS Collaboration, R. Abusaidi et al., Phys. Rev. Lett. 84 (2000) 5699.
- [4] EDELWEISS Collaboration, A. Benoit et al., Phys. Lett. B513 (2001) 15.
- [5] IGEX Collaboration, A. Morales et al., hep-ex/0110061.
- [6] D.G. Cerdeño, S. Khalil and C. Muñoz, Proceedings of CICHEP Conference in Cairo, Rinton Press (2001) 214, hep-ph/0105180.
- [7] A. Bottino, F. Donato, N. Fornengo and S. Scopel, Phys. Rev. D59 (1999) 095004.
- [8] E. Accomando, R. Arnowitt, B. Dutta and Y. Santoso, Nucl. Phys. B585 (2000) 124.
- [9] A. Corsetti and P. Nath, . Phys. Rev. D64 (2001) 125010.
- [10] R. Arnowitt and B. Dutta, hep-ph/0112157.
- [11] E. Gabrielli, S. Khalil, C. Muñoz and E. Torrente-Lujan, Phys. Rev. D63 (2001) 025008.

- [12] D. Bailin, G.V. Kraniotis and A. Love, Phys. Lett. B491 (2000) 161.
- [13] D.G. Cerdeño, E. Gabrielli, S. Khalil, C. Muñoz and E. Torrente-Lujan, Nucl. Phys. B603 (2001) 231.
- [14] For a review, see, A. Brignole, L.E. Ibanez and C. Muñoz, in the book ‘Perspectives on Supersymmetry’, World Scientific Publ. Co. (1998) 125, hep-ph/9707209.
- [15] S. Ambrosiano, A. Dedes, S. Heinemeyer, S. Su and G. Weiglein, Nucl. Phys. B624 (2002) 3.
- [16] The ALEPH, DELPHI, L3 and OPAL Collaborations, and the LEP Higgs working group, hep-ex/0107030.
- [17] S. Heinemeyer, W. Hollik and G. Weiglein, Comp. Phys. Comm. 124 (2000) 76; hep-ph/0002213; M. Frank, S. Heinemeyer, W. Hollik and G. Weiglein, hep-ph/0202166.
- [18] Joint LEP 2 supersymmetry working group, http://lepsusy.web.cern.ch/lepsusy/www/inos_moriond01/charginos_pub.html
- [19] Joint LEP 2 supersymmetry working group, http://alephwww.cern.ch/~ganis/SUSYWG/SLEP/sleptons_2k01.html
- [20] CLEO Collaboration, S. Chen et al., hep-ex/0108032.
- [21] BELLE Collaboration, H. Tajima, hep-ex/0111037.
- [22] K. Chetyrkin, M. Misiak and M. Munz, Phys. Lett. B400 (1997) 206, Erratum-ibid. B425 (1997) 414; P. Gambino and M. Misiak, Nucl. Phys. B611 (2001) 338.
- [23] S. Bertolini, F. Borzumati, A. Masiero and G. Ridolfi, Nucl. Phys. B353 (1991) 591; E. Gabrielli and U. Sarid, Phys. Rev. Lett. 79 (1997) 4752.
- [24] Muon $g - 2$ Collaboration, H.N. Brown et al., Phys. Rev. Lett. 86 (2001) 2227.
- [25] M. Knecht and A. Nyffeler, hep-ph/0111058; M. Knecht, A. Nyffeler, M. Perrottet and E. de Rafael, Phys. Rev. Lett. 88 (2002) 071802; Hayakawa and Kinoshita, hep-ph/0112102; I. Blokland, A. Czarnecki and K. Melnikov, Phys. Rev. Lett. 88 (2002) 071803; J. Bijnens, E. Pallante and J. Prades, Nucl. Phys. B626 (2002) 410.
- [26] J. Bijnens, E. Pallante and J. Prades, Phys. Rev. Lett. 75 (1995) 1447, Erratum-ibid. 75 (1995) 3781, Nucl. Phys. B474 (1996) 379; M. Hayakawa, T. Kinoshita and A.I. Sanda, Phys. Rev. Lett. 75 (1995) 790, Phys. Rev D54 (1996) 3137; M. Hayakawa and T. Kinoshita, Phys. Rev D57 (1998) 465.
- [27] See, e.g., A. Kudo and M. Yamaguchi, Phys. Lett. B516 (2001) 151. hep-ph/0103272, and references therein.

- [28] See, e.g., S. Khalil, C. Muñoz and E. Torrente-Lujan, hep-ph/0202139, and references therein.
- [29] J. Ellis, A. Ferstl and K. Olive, Phys. Lett. B481 (2000) 304.
- [30] J. Ellis, A. Ferstl and K. Olive, hep-ph/0111064.
- [31] P. Belli, R. Cerulli, N. Fornengo and S. Scopel, hep-ph/0203242.
- [32] H.V. Klapdor-Kleingrothaus, L. Baudis, G. Heusser, B. Majorovits and H. Paes, hep-ph/9910205.
- [33] M.E. Gómez and J.D. Vergados, Phys. Lett. B512 (2001) 252.
- [34] D.G. Cerdeño, E. Gabrielli, S. Khalil, C. Muñoz and E. Torrente-Lujan, Phys. Rev. D64 (2001) 093012.